



Cite this: *Chem. Commun.*, 2019, 55, 4534

Received 20th February 2019,
Accepted 20th March 2019

DOI: 10.1039/c9cc01448a

rsc.li/chemcomm

Synthesis of cAAC stabilized biradical of “Me₂Si” and “Me₂SiCl” monoradical from Me₂SiCl₂ – an important feedstock material†

Soumen Sinhababu,^a Subrata Kundu,^a Mujahuddin M. Siddiqui,^a Alexander N. Paesch,^a Regine Herbst-Irmer,^a Brigitte Schwederski,^b Pinaki Saha,^c Lili Zhao,^c Gernot Frenking,^d Wolfgang Kaim,^b Dietmar Stalke^b and Herbert W. Roesky^b

The cyclic alkyl(amino) carbene (cAAC) coordinated biradical of dimethylsilicon was isolated as (cAAC)₂Me₂Si (**1**), (cAAC = C(CH₂)(CMe₂)₂N-2,6-i-Pr₂C₆H₃), synthesized from the reduction of Me₂SiCl₂ using two equivalents of KC₈ in the presence of two equivalents of cAAC. The reduction of Me₂SiCl₂ by one equivalent of KC₈ in the presence of one equivalent of cAAC resulted in the stable dimethylsiliconchloride monoradical (cAAC)Me₂SiCl (**2**).

Radicals and biradicals have attracted considerable attention in chemistry and material science due to their unique optical, magnetic and electronic properties.¹ In 1915 Schlenk isolated the first paramagnetic biradical from the reaction of bis-diphenylbenzyl dichloride with a copper–tin alloy.^{2a} Most of the radicals are unstable and are short-lived.^{2b–d} However, they can be isolated and stored at room temperature in a pure form using either thermodynamic or kinetic stabilization.^{3,4} Several stable carbon and silicon centered biradicals are known.⁵ Carbon centered 1,3-biradicals are proposed to be key reactive intermediates in certain chemical reactions.⁶ Limited examples of four-membered heterocyclic 1,3-biradicals of cyclobutane type were reported.⁷ Recently, we have synthesized air stable carbon centered 1,3-biradical (cAAC)₂SiCl₂ (**I**)⁸ (Chart 1) from the reaction of NHC → SiCl₂ (NHC = N-heterocyclic carbene) with a cyclic alkyl(amino) carbene. Furthermore, our group successfully synthesized cAAC stabilized SiX₂ (X = H, F) (Chart 1) bridged

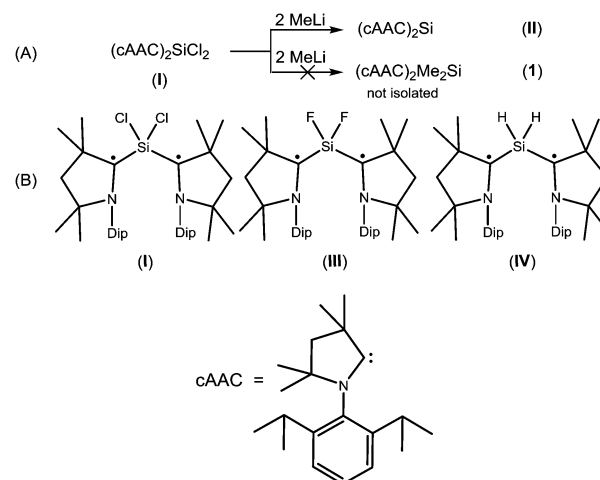


Chart 1 (A) The unsuccessful attempted synthesis of (cAAC)₂Me₂Si (**1**); (B) structurally characterized stable biradicals containing SiX₂ (X = Cl, F, H) moiety^{8–10}

1,3-biradicals, which are stable at room temperature for more than three months under inert atmosphere. The elusive SiF₂ bridged biradical (cAAC)₂SiF₂ (**III**) (Chart 1) was synthesized from the reduction of (cAAC)SiF₄ by using two equivalents of KC₈ in the presence of one equivalent of cAAC.⁹ While, (cAAC)₂SiH₂ (**IV**) (Chart 1) was prepared from the reduction of H₂SiI₂ with two equivalents of KC₈, in the presence of two equivalents of cAAC.¹⁰ After the successful isolation of cAAC stabilized SiX₂ (X = H, Cl, F) bridged 1,3-biradicals, the isolation of SiMe₂ analogues (cAAC)₂Me₂Si (**1**) was a prominent missing link in this class of compounds. Dimethyl silicon is not stable at room temperature and polymerises to (SiMe₂)_n. In our earlier synthetic route, we tried to isolate **1**, by the reaction of (cAAC)₂SiCl₂ with 2 equivalents of MeLi by the nucleophilic substitution method.¹¹ To our surprise, MeLi functioned as a reducing agent leading to the isolation of dehalogenated biradicaloid (cAAC)₂Si (**II**).¹² Me₂SiCl₂ is the most important feedstock material in the industry for the preparation of silicones.¹³ We envisaged an

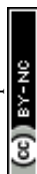
^a Institut für Anorganische Chemie, Universität Göttingen, Tammannstrasse 4, 37077 Göttingen, Germany. E-mail: hroesky@gwdg.de, dstalke@chemie.uni-goettingen.de

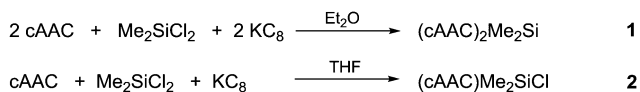
^b Universität Stuttgart, Institut für Anorganische Chemie, 70569 Stuttgart, Germany. E-mail: kaim@iac.uni-stuttgart.de

^c Institute of Advanced Synthesis, School of Chemistry and Molecular Engineering, Jiangsu National Synergetic Innovation Center for Advanced Materials, Nanjing Tech University, Nanjing 211816, China

^d Universität Marburg, Fachbereich Chemie, Hans-Meerwein-Strasse, 35032 Marburg, Germany

† Electronic supplementary information (ESI) available: Including experimental section, computational details and details of X-ray structural analysis. CCDC 1894458 (**1**) and 1894459 (**2**). For ESI and crystallographic data in CIF or other electronic format see DOI: 10.1039/c9cc01448a



Scheme 1 Synthesis of **1** and **2**.

alternative route to the isolation of **1** by the reduction of commercially available Me_2SiCl_2 . Herein, we report a one step synthesis of the biradical $(\text{cAAC})_2\text{Me}_2\text{Si}$ (**1**) and monoradical $(\text{cAAC})\text{Me}_2\text{SiCl}$ (**2**) by the reduction of Me_2SiCl_2 with KC_8 .

Both the compounds **1** and **2** were fully characterized by X-ray crystallography and EPR spectroscopy. Compound **1** was prepared by reduction of Me_2SiCl_2 using KC_8 in a 1:2 molar ratio in the presence of two equivalents of cAAC (Scheme 1; for details, see ESI†). ^1H NMR spectrum of compound **1** shows broad resonance indicating the radical nature. **1** has been characterized by EPR spectroscopy, LIFDI mass spectrometry, elemental analysis and single crystal structure analysis. **1** is stable in an inert atmosphere for more than 6 months in the solid state. It is thermally stable at room temperature and decomposes at 148°C . The UV/Vis spectrum of **1** in a hexane solution shows an absorption band at 575 nm. The LIFDI mass spectrum in toluene exhibits a peak at 629.6 m/z for $[\text{M}]^+$. Single crystals of **1** suitable for X-ray diffraction analysis were grown from hexane solution at -26°C .

A stable radical containing the Me_2SiCl group has not been reported so far. Equivalent amounts of cAAC, Me_2SiCl_2 and KC_8 , respectively, treated in THF at -90°C resulted in the desired monoradical product $(\text{cAAC})\text{Me}_2\text{SiCl}$ (**2**) as orange coloured crystals in 68% yield (Scheme 1).

2 was characterized by EPR spectroscopy, LIFDI mass spectrometry, elemental analysis and single crystal structure analysis. The LIFDI mass spectrum in toluene exhibits a molecular ion peak at 378.2 m/z . The UV/Vis spectrum of **2** in hexane shows an absorption band at 435 nm. The EPR spectra of compounds **1** and **2** were recorded in hexane solution at room temperature. It must be mentioned that efforts to isolate such type of radical species with NHC were not successful.

1 crystallizes in the monoclinic space group $C2/c$. The molecular structure of **1** (Fig. 1) reveals the central Si atom to be distorted tetrahedrally coordinated by four carbon atoms. The Si–Me bond lengths [1.8768(13) and 1.8800(13) Å] are similar to the $\text{C}_{\text{AAC}}\text{–Si}$ distances [1.8814(13) and 1.8829(13) Å] and to the distances reported in the literature.^{10,14} The C2–Si1–C2A bond angle ($116.86(5)^\circ$) is widened due to the steric hindrance of the bulky cAAC ligands, but nevertheless smaller than in the silylone $(\text{cAAC})_2\text{Si}$ of $119.10(1)^\circ$.^{12b}

2 crystallizes in the orthorhombic space group $Pbca$. The molecular structure (Fig. 2) reveals the silicon atom to be tetra-coordinated with three carbon and one chlorine atom. The Si–Cl bond length (2.1228(5) Å) is longer than those in $(^{\text{Me}}\text{cAAC})\text{SiCl}_3$ (2.0396(4)–2.0864(3) Å).¹⁵

The EPR spectrum of **1** is dominated by a 1:1:1 triplet of 4.65 G (Fig. 3), attributed to the coupling of the unpaired electron with one ^{14}N atom ($I = 1$). This splitting^{9,10,15} suggests localized spin at only one of the two equivalent cAAC groups

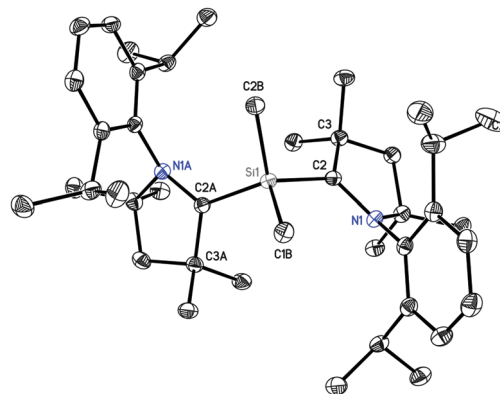


Fig. 1 Crystal structure of **1**. Hydrogen atoms are omitted for clarity. Thermal ellipsoid plot is drawn at 50% probability. Selected experimental bond lengths [Å] and angles [$^\circ$]. Calculated values at BP86/def2-TZVP are given in brackets: Si1–C2B, 1.8768(13) [1.891]; Si1–C1B, 1.8800(13) [1.891]; Si1–C2, 1.8814(13) [1.886]; Si1–C2A, 1.8829(13) [1.886]; C2B–Si1–C1B, $106.55(6)$ [106.6]; C2B–Si1–C2, $108.33(6)$ [108.7]; C1B–Si1–C2, $107.98(6)$ [108.9]; C2B–Si1–C2A, $108.40(6)$ [108.7]; C1B–Si1–C2A, $108.27(6)$ [108.7]; C2–Si1–C2A, $116.86(5)$ [114.9].

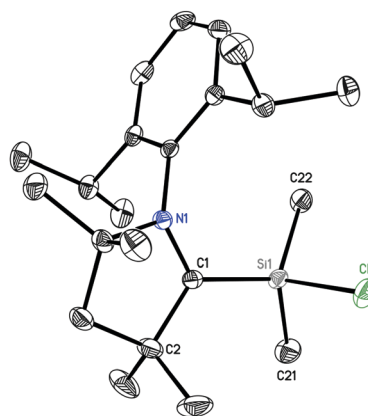


Fig. 2 Crystal structure of **2**. Hydrogen atoms are omitted for clarity. Thermal ellipsoid plot is drawn at 50% probability. Selected experimental bond lengths [Å] and angles [$^\circ$]. Calculated values at BP86/def2-TZVP are given in brackets: Si1–C1, 1.8323(12) [1.841]; Si1–C22, 1.8633(13) [1.878]; Si1–C21, 1.8645(13) [1.876]; Si1–Cl1, 2.1228(5) [2.138]; C1–Si1–C22, $117.67(6)$; C1–Si1–C21, $113.16(6)$; C22–Si1–C21, $108.22(6)$; C1–Si1–Cl1, $108.56(4)$ [108.1]; C22–Si1–Cl1, $104.05(4)$ [104.5]; C21–Si1–Cl1, $103.91(5)$ [105.0].

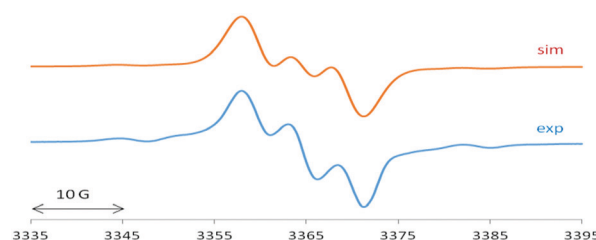


Fig. 3 EPR spectrum of **1** with computer simulation (top). For parameters see main text.

connected to the silicon atom which exhibits a typically ^{29}Si isotope coupling^{9,10,15} of 27.5 G (^{29}Si : $I = 1/2$, 4.7% nat. abundance).



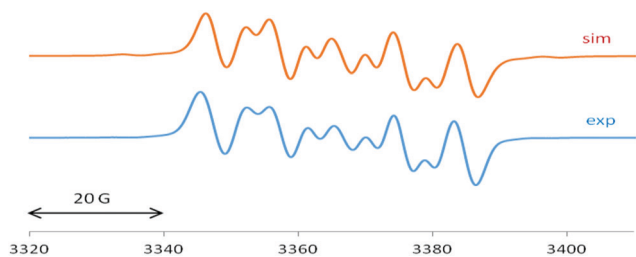


Fig. 4 EPR spectrum of **2** with computer simulation (top). For parameters see main text.

2 exhibits an EPR spectrum (Fig. 4) with similar ^{14}N and ^{29}Si values of 5.4 G and 25 G, respectively, in addition to a sizeable chlorine splitting from the isotopes ^{35}Cl ($I = 3/2$, 75.8% nat. abundance: 8.9 G) and ^{37}Cl ($I = 3/2$, 24.2%: 7.4 G). Such Cl(Si) coupling has been noted before for related silicon radicals.¹⁵

We carried out quantum chemical calculations using density functional theory at the BP86/def2-TZVP level²³ in order to analyze the electronic structure of compounds **1** and **2**. Fig. 1 and 2 shows also the computed bond lengths and angles of the optimized geometries of the two molecules, which are in excellent agreement with the experimental data. The calculations suggest that **1** has an electronic triplet ground state whereas **2** is a doublet, which concurs with the EPR results. Fig. 5 shows the spin density distribution of the two molecules. The unpaired electrons in **1** and **2** are mainly located at the nitrogen atoms and the carbene carbon atoms of the cAAC moieties.

We further analyzed the nature of the cAAC–Si bonds in **1** and **2** with the EDA-NOCV method.²⁴ Table S1 (ESI[†]) shows the numerical results. The calculations for **1** were carried out using the cAAC fragments in the electronic triplet state, which gives an overall quintet state for the (cAAC)₂ ligand, and the SiMe₂ moiety in the triplet state. For compound **2** we took the cAAC ligand in the triplet state and the SiMe₂Cl fragment in the doublet state. The choice of the open-shell fragments corresponds to electron-sharing single bonds. Comparative calculations using an electronic singlet state spin for the cAAC ligands, which correspond to dative bonds cAAC → Si, gave significantly larger orbital values ΔE_{orb} (see Tables S2 and S3 in ESI[†]). It has been shown in previous studies that the orbital values ΔE_{orb} are a probe for the choice of the best fragments.²⁵

The data in Table S1 (ESI[†]) show that the covalent orbital interactions ΔE_{orb} have nearly equal strength as the Coulomb attraction. There are two major orbital contributions $\Delta E_{\text{orb}(1)}$

and $\Delta E_{\text{orb}(2)}$ in compound **1** and one dominant term $\Delta E_{\text{orb}(1)}$ in **2**, which come from pairwise orbital interactions between the chosen fragments. Fig. S5 (ESI[†]) shows the plots of the associated deformation densities $\Delta\rho$, which illustrate the charge flow that is connected to the orbital interactions. The color code of the charge flow indicates the direction red → blue. The complete list of the deformation densities $\Delta\rho$ and the connected fragment orbitals are shown in Fig. S3 and S4 of ESI[†]. It becomes obvious that $\Delta E_{\text{orb}(1)}$ in compound **1** is due to the interaction between the singly occupied σ orbital (SOMO) of SiMe₂ with the in-phase (+, +) combination of the π -type²⁶ SOMO of (cAAC)₂, where the net charge flow is from SiMe₂ → (cAAC)₂. The stabilization energy $\Delta E_{\text{orb}(2)}$ in compound **1** comes from the interaction of the π SOMO of SiMe₂ with the out-of-phase (+, –) combination of the σ -type²⁶ SOMO of (cAAC)₂. The dominant orbital interaction $\Delta E_{\text{orb}(1)}$ in compound **2** is due to the interaction between the σ SOMO of SiClMe₂ with the σ SOMO of cAAC. The direction of the charge flow between the ligands is in agreement with the calculated partial charges by the NBO²⁷ method. The computed charges q at the BP86/def2-TZVP level are $q(\text{SiMe}_2) = +0.82 e$ for **1** and $q(\text{SiClMe}_2) = +0.36 e$ for **2**. Thus, the cAAC ligand in **1** and **2** acts as an acceptor rather than donor.

In summary, we report on the synthesis of 1,3-biradical containing Me₂Si moiety using cAAC as ligand. Moreover we isolated the monoradical (cAAC)Me₂SiCl. Theoretical investigations and EPR spectra of both compounds have been reported. The calculations suggest that **1** has an electronic triplet ground state whereas **2** is a doublet.

Crystal structure determination. Single crystals were selected and covered with perfluorinated polyether oil on a microscope slide.¹⁶ An appropriate crystal was selected using a polarize microscope, mounted on the tip of a MiTeGen[®] MicroMount, fixed to a goniometer head and shock cooled by the crystal cooling device. The data of **1** and **2** were collected from shock-cooled crystals at 100(2) K on a BRUKER D8 three circle diffractometer equipped with an INCOATEC Mo microsource with mirror optics (MoK α radiation, $\lambda = 0.71073 \text{ \AA}$) and smart APEX II detector. They were integrated with SAINT.¹⁷ A multi-scan absorption correction and a 3λ correction¹⁸ was applied using SADABS.¹⁹ The structure were solved by direct methods (SHELXT)²⁰ and refined by full-matrix least-squares methods against F^2 (SHELXL)²¹ in the graphical user interface ShelXle.²² CCDC 1894458 (**1**) and 1894459 (**2**).[†]

H. W. R. is thankful to the DFG for financial support (RO 224/68-1). D. S. thanks the Danish National Research Foundation (DNRF93) funded Centre for Materials Crystallography (CMC) for partial support. We thank Dr A. C. Stückl for EPR measurements. G. F. and L. Z. thank Nanjing Tech University (Grant No. 39837132 and 39837123) and SICAM Fellowship from Jiangsu National Synergetic Innovation Center for Advanced Materials. L. Z. acknowledges the financial support from National Natural Science Foundation of China (Grant No. 21703099), Natural Science Foundation of Jiangsu Province (Grant No. BK20170964), and the high performance center of Nanjing Tech University for supporting the computational resources.

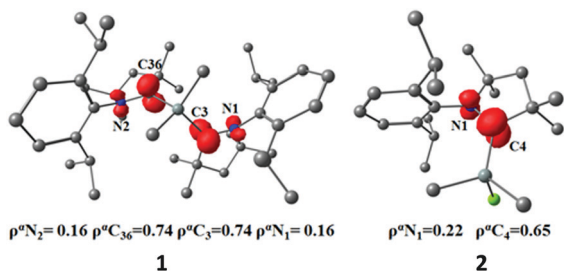


Fig. 5 Spin density at the of compounds **1** and **2** at the BP86/def2-TZVP level.



Conflicts of interest

There are no conflicts to declare.

Notes and references

- (a) M. Abe, *Chem. Rev.*, 2013, **113**, 7011–7088; (b) Y. Morita, S. Nishida, T. Murata, M. Moriguchi, A. Ueda, M. Satoh, K. Arifuku, K. Sato and T. Takui, *Nat. Mater.*, 2011, **10**, 947–951; (c) I. Ratera and J. Veciana, *Chem. Soc. Rev.*, 2012, **41**, 303–349; (d) Z. Zeng, X. Shi, C. Chi, J. T. L. Navarrete, J. Casado and J. Wu, *Chem. Soc. Rev.*, 2015, **44**, 6578–6596.
- (a) W. Schlenk and M. Brauns, *Chem. Ber.*, 1915, **48**, 661–669; (b) G. Porter and M. W. Windsor, *Nature*, 1957, **180**, 187–188; (c) E. G. Janzen and B. J. Blackburn, *J. Am. Chem. Soc.*, 1968, **90**, 5909–5910; (d) M. Abe, W. Adam and W. M. Nau, *J. Am. Chem. Soc.*, 1998, **120**, 11304–11310.
- Organic and organometallic monoradicals: (a) M. M. Hansmann, M. Melaimi and G. Bertrand, *J. Am. Chem. Soc.*, 2017, **139**, 15620–15623; (b) D. Mandal, R. Dolai, N. Chrysochos, P. Kalita, R. Kumar, D. Dhara, A. Maiti, R. S. Narayanan, G. Rajaraman, C. Schulzke, V. Chandrasekhar and A. Jana, *Org. Lett.*, 2017, **19**, 5605–5608; (c) D. Rottschäfer, B. Neumann, H.-G. Stammer, M. van Gastel, D. M. Andrada and R. S. Ghadwal, *Angew. Chem., Int. Ed.*, 2018, **57**, 4765–4768; (d) S. Styra, M. Melaimi, C. E. Moore, A. L. Rheingold, T. Augenstein, F. Breher and G. Bertrand, *Chem. – Eur. J.*, 2015, **21**, 8441–8446; (e) S. Kundu, S. Sinhababu, S. Dutta, T. Mondal, D. Koley, B. Dittrich, B. Schwederski, W. Kaim, A. C. Stückl and H. W. Roesky, *Chem. Commun.*, 2017, **53**, 10516–10519; (f) M. M. Siddiqui, S. K. Sarkar, S. Sinhababu, P. N. Ruth, R. Herbst-Irmer, D. Stalke, M. Ghosh, M. Fu, L. Zhao, D. Casanova, G. Frenking, B. Schwederski, W. Kaim and H. W. Roesky, *J. Am. Chem. Soc.*, 2019, **141**, 1908–1912.
- Organic and organometallic biradicals: (a) M. M. Hansmann, M. Melaimi, D. Munz and G. Bertrand, *J. Am. Chem. Soc.*, 2018, **140**, 2546–2554; (b) D. Rottschäfer, N. K. T. Ho, B. Neumann, H.-G. Stammer, M. van Gastel, D. M. Andrada and R. S. Ghadwal, *Angew. Chem., Int. Ed.*, 2018, **57**, 5838–5842; (c) D. Rottschäfer, B. Neumann, H.-G. Stammer, D. M. Andrada and R. S. Ghadwal, *Chem. Sci.*, 2018, **9**, 4970–4976; (d) K. C. Mondal, B. Dittrich, B. Maity, D. Koley and H. W. Roesky, *J. Am. Chem. Soc.*, 2014, **136**, 9568–9571; (e) T. Nozawa, M. Nagata, M. Ichinohe and A. Sekiguchi, *J. Am. Chem. Soc.*, 2011, **133**, 5773–5775.
- M. Abe, J. Ye and M. Mishima, *Chem. Soc. Rev.*, 2012, **41**, 3808–3820.
- (a) W. G. Bentrude, S.-G. Lee, K. Akutagawa, W.-Z. Ye and Y. Charbonnel, *J. Am. Chem. Soc.*, 1987, **109**, 1577–1579; (b) W. Adam, G. Reinhard, H. Platsch and J. Wirz, *J. Am. Chem. Soc.*, 1990, **112**, 4570–4571; (c) M. Sakamoto, H. Kawanishi, T. Mino and T. Fujita, *Chem. Commun.*, 2008, 2132–2133.
- (a) J. Bresien, A. Hinz, A. Schulz and A. Villinger, *Dalton Trans.*, 2018, **47**, 4433–4436; (b) K. Takeuchi, M. Ichinohe and A. Sekiguchi, *J. Am. Chem. Soc.*, 2011, **133**, 12478–12481; (c) H. Cox, P. B. Hitchcock, M. F. Lappert and L. J.-M. Pierssens, *Angew. Chem., Int. Ed.*, 2004, **43**, 4500–4504; (d) C. Cui, M. Brynda, M. M. Olmstead and P. P. Power, *J. Am. Chem. Soc.*, 2004, **126**, 6510–6511; (e) D. Scheschke, H. Amii, H. Gornitzka, W. W. Schoeller, D. Bourissou and G. Bertrand, *Science*, 2002, **295**, 1880–1881; (f) T. Baumgartner, D. Gudat, M. Nieger, E. Niecke and T. J. Schiffer, *J. Am. Chem. Soc.*, 1999, **121**, 5953–5960; (g) E. Niecke, A. Fuchs, F. Baumeister, M. Nieger and W. W. Schoeller, *Angew. Chem., Int. Ed. Engl.*, 1995, **34**, 555–557.
- K. C. Mondal, H. W. Roesky, M. C. Schwarzer, G. Frenking, I. Tkach, H. Wolf, D. Kratzert, R. Herbst-Irmer, B. Niepötter and D. Stalke, *Angew. Chem., Int. Ed.*, 2013, **52**, 1801–1805.
- S. Sinhababu, S. Kundu, A. N. Paesch, R. Herbst-Irmer, D. Stalke, I. Fernandez, G. Frenking, A. C. Stückl, B. Schwederski, W. Kaim and H. W. Roesky, *Chem. – Eur. J.*, 2018, **24**, 1264–1268.
- S. Kundu, P. P. Samuel, S. Sinhababu, A. V. Luebben, B. Dittrich, D. M. Andrada, G. Frenking, A. C. Stückl, B. Schwederski, A. Paretzki, W. Kaim and H. W. Roesky, *J. Am. Chem. Soc.*, 2017, **139**, 11028–11031.
- K. C. Mondal, P. P. Samuel, M. Tretiakov, A. P. Singh, H. W. Roesky, A. C. Stückl, B. Niepötter, E. Carl, H. Wolf, R. Herbst-Irmer and D. Stalke, *Inorg. Chem.*, 2013, **52**, 4736–4743.
- (a) K. C. Mondal, H. W. Roesky, M. C. Schwarzer, G. Frenking, B. Niepötter, H. Wolf, R. Herbst-Irmer and D. Stalke, *Angew. Chem., Int. Ed.*, 2013, **52**, 2963–2967; (b) B. Niepötter, R. Herbst-Irmer, D. Kratzert, P. P. Samuel, K. C. Mondal, H. W. Roesky, P. Jerabek, G. Frenking and D. Stalke, *Angew. Chem., Int. Ed.*, 2014, **53**, 2766–2770.
- H.-H. Moretto, M. Schulze and G. Wagner, *Silicones, in Ullmann's Encyclopedia of Industrial Chemistry*, Wiley-VCH Verlag GmbH & Co. KGaA, 2000, pp. 675–712.
- (a) S. Kundu, S. Sinhababu, M. M. Siddiqui, A. V. Luebben, B. Dittrich, T. Yang, G. Frenking and H. W. Roesky, *J. Am. Chem. Soc.*, 2018, **140**, 9409–9412; (b) M. M. Siddiqui, S. Sinhababu, S. Dutta, S. Kundu, P. N. Ruth, A. Münch, R. Herbst-Irmer, D. Stalke, D. Koley and H. W. Roesky, *Angew. Chem., Int. Ed.*, 2018, **57**, 11776–11780.
- S. Roy, A. C. Stückl, S. Demeshko, B. Dittrich, J. Meyer, B. Maity, D. Koley, B. Schwederski, W. Kaim and H. W. Roesky, *J. Am. Chem. Soc.*, 2015, **137**, 4670–4673.
- (a) T. Kottke and D. Stalke, *J. Appl. Crystallogr.*, 1993, **26**, 615–619; (b) T. Kottke, R. J. Lagow and D. Stalke, *J. Appl. Crystallogr.*, 1996, **29**, 465–468; (c) D. Stalke, *Chem. Soc. Rev.*, 1998, **27**, 171–178; (d) see the video at http://www.stalke.chemie.uni-goettingen.de/virtuelles_labor/special/22_de.html.
- SAINT v8.30C in BRUKER APEX II, BRUKER AXS Inst. Inc., Madison, USA, 2014.
- L. Krause, R. Herbst-Irmer and D. Stalke, *J. Appl. Crystallogr.*, 2015, **48**, 1907–1913.
- L. Krause, R. Herbst-Irmer, G. M. Sheldrick and D. Stalke, *J. Appl. Crystallogr.*, 2015, **48**, 3–10.
- G. M. Sheldrick, *Acta Crystallogr., Sect. A: Found. Adv.*, 2015, **71**, 3–8.
- G. M. Sheldrick, *Acta Crystallogr., Sect. C: Struct. Chem.*, 2015, **71**, 3–8.
- C. B. Hübschle, G. M. Sheldrick and B. Dittrich, *J. Appl. Crystallogr.*, 2011, **44**, 1281–1284.
- The details of the theoretical methods are described in the ESI†.
- M. P. Mitoraj, A. Michalak and T. Ziegler, *J. Chem. Theory Comput.*, 2009, **5**, 962–975.
- Recent representative examples: (a) C. Mohapatra, S. Kundu, A. N. Paesch, R. Herbst-Irmer, D. Stalke, D. M. Andrada, G. Frenking and H. W. Roesky, *J. Am. Chem. Soc.*, 2016, **138**, 10429–10432; (b) D. M. Andrada, J. L. Casals-Sainz, A. M. Pendas and G. Frenking, *Chem. – Eur. J.*, 2018, **24**, 9083–9089; (c) L. Zhao, M. Hermann, N. Holzmann and G. Frenking, *Coord. Chem. Rev.*, 2017, **344**, 163–204.
- The symmetry assignments σ and π refer to the local symmetry of the fragments.
- C. R. Landis and F. Weinhold, *Valency and Bonding: A Natural Bond Orbital Donor-Acceptor Perspective*, Cambridge University Press, Cambridge, 2005.

